Research Article | Vol. 26, No. 21 | 15 Oct 2018 | OPTICS EXPRESS 27368
Optics EXPRESS

Helical pitch-dependent electro-optics of optically high transparent nano-phase separated liquid crystals

SRINIVAS PAGIDI,[1] RAMESH MANDA,[1] YOUNG JIN LIM,[1] SEONG MIN SONG,[1] HYESUN YOO,[1] JONG HOON WOO,[1] YI-HSIN LIN,[2] AND SEUNG HEE LEE,[1*]

[1]*Applied Materials Institute for BIN Convergence, Department of BIN Convergence Technology and Department of Polymer Nano Science and Technology, Chonbuk National University, Jeonju, Jeonbuk, 561-756, South Korea*
[2]*Department of Photonics, National Chiao Tung University, Hsinchu 30010, Taiwan*
**lsh1@chonbuk.ac.kr*

Abstract: Feeble light leakage in a dark state of conventional optically isotropic liquid crystal (OILC) device has a strong impact on the contrast ratio of a liquid crystal (LC) device. In order to overcome such intrinsic problem, we proposed an OILC in which the LC directors inside droplets are twisted by introducing chirality. The light leakage is effectively suppressed by matching the refractive indices between LC and polymer matrix; consequently, we achieved a high contrast ratio, 1:1401. Interestingly, the on-state transmittance is enhanced by ~49% compared to conventional OILC. The response time was also improved and the hysteresis was suppressed to be negligible. The improved electro-optic performances of the proposed OILC device would give diverse applications in upcoming flexible display and various photonic devices.

1. Introduction

Optically isotropic liquid crystal (OILC) defines as an optical medium, consisting of either pure liquid crystals (LC) or a complex system of LC and polymeric mixture, exhibits optical isotropy to the incident light. In recent days, the OILC have attracted much attention from the fundamental and technological point of view because of their nano-structured LC exhibiting a superior performance over the conventional LC modes for liquid crystal display (LCD). Owing to the remarkable electro-optics such as fast response time, wide viewing angle, wide enough optically isotropic range, alignment layer free, cell gap insensitive, and adaptability to flexibility makes them more attractive for future display and photonic applications [1–6]. OILCs are broadly classified into two categories, one is blue phase liquid crystals (BPLC) and another is nano-phase-separated liquid crystals (NPSLC). Both of these exhibit the optically isotropic phase at field-off state and induce birefringence when field is applied. This phenomenon can be explained by the well-known Kerr effect. The great advantage of BPLC is that a higher Kerr constant can be achieved. However, the BPLC is currently suffering from few drawbacks such as narrow phase range, hysteresis, and high operating voltage [7–9]. Also, the strong optical activity, due to locally twisted structures limits the isotropic nature. Another OILC material is NPSLC which shows an efficient optically isotropic phase while avoiding drawbacks of BPLC. In addition, the NPSLC provides a wider operating phase range and capable to reduce the hysteresis to zero.

Aside from several approaches reported to prepare the NPSLC, the polymerization induced phase separation is the most versatile and efficient method at which the high amount of photo-curable monomers added to the LC and then formation of smaller LC droplets, <350 nm, in a polymer matrix is obtained after phase separation [4,10,11]. Each droplet in a

#341943 https://doi.org/10.1364/OE.26.027368
Journal © 2018 Received 9 Aug 2018; revised 28 Sep 2018; accepted 29 Sep 2018; published 4 Oct 2018

Optics EXPRESS

polymer matrix orient independently and the optically isotropic phase is realized when a visible light passing through [12–14]. The electro-optical properties are governed by the LC molecules distributed inside the droplet and how they interact with polymer walls. The great advantage of NPSLC is a variety of droplet structures can be fabricated through adjusting experimental parameters freely on phase separation process to achieve desired properties. However, formation of few bigger droplets in 10 μm thick film creates a slight light leakage from isotropic phase which limits the device performance with low contrast ratio [4,6]. The straight forward way to overcome this issue would be increasing the monomer concentration and decreasing possibility bigger droplet formation. But it leads to the higher operating voltage which is again not a desirable property. On the other hand, the bipolar structure of the LC droplet, which is the most possible structure for smaller droplets, would also cause to the light leakage by altering the LC orientation at the poles and rest of the droplet [15,16]. The fabrication of smaller non-bipolar LC droplet which could require less voltage to switch is rather difficult and challenging.

In the present report, we have demonstrated an OILC phase with helical/twisted droplets by introducing chiral dopant to the conventional NPSLC. Herein, we prepared various OILC mixtures with varying pitch length and systematically investigated a helical twist impact on electro-optical properties. Interestingly, the helical droplets are effectively suppressed the light leakage and, consequently, a high contrast ratio was achieved. We also found that the light leakage is linearly proportional to the pitch length. In addition, the on-state transmittance is also strongly affected by the helical twist generated inside droplets. The on-state transmittance is enhanced by ~49% for 1.5 μm pitch length sample with compare to conventional OILC. In addition, the decay response time was drastically improved with negligible hysteresis. The electro-optical and surface morphological properties have been studied in detailed.

2. Principle of operation

The schematic of LC director orientation in conventional OILCs (conventional-OILC) and the proposed twisted OILCs (twisted-OILC) has been shown in Fig. 1. The director distribution inside the droplet was schematically shown in inset of both cases. The sample is sandwiched between two glass substrates: the bottom one is coated with electrodes while the top one is not coated any electrodes. In conventional-OILC, the sizes of the LC droplets are usually smaller than the visible wavelength and the LC molecular orientation inside the droplets is expected to be a bipolar configuration due to strong anchoring energy, as shown in inset of Fig. 1(a). Assuming the LC droplet is spherical in shape and tangentially anchored to the polymer wall, the nematic director field follows the path of polymer walls at surface of the droplet while follows straight line connecting two poles at center of the droplet. Overall, the line connecting two poles would be a symmetric axis of the droplet therefore defined as director. In a macroscopic viewpoint, the director distribution of the sample is random. Nevertheless, the alteration of director field at the droplet surface and bulk generates to refractive index mismatch with polymer network that result in a slight light scattering. In addition, based on our previous results we found that a few LC droplets those are larger than the expected i.e. >350 nm resulted in a weak scattering or opaque state of the device [4,17–19].

According to the Rayleigh-Gans (RG) scattering theory, the scattering occurs when the light passing through the medium experiences change in refractive index. Implying the same scenario to NPSLC, the intensity of scattered light is determined by the equation $B = N\sigma_{avg}d$. Here, N is the number of scattering centers exists in the OILC film, d is thickness of the film, and σ_{avg} is an average cross-sectional area that would cause refractive index change. The average cross-sectional area causing scattering $\left(\sigma_{avg}\right)$ can be expressed as [20],

Optics EXPRESS

$$\sigma_{avg} \propto |m-1|^2 \Gamma^4 R^6, \quad (1)$$

where m is a ratio of the refractive indices of nematic LC (n_{LC}) to polymer (n_p) matrix (i.e. n_{LC}/n_P), Γ is a wave number ($2\pi n_p/\lambda, \lambda$ is wavelength of the incident light), and R is the radius of a LC droplet. When the n_{LC} is exactly matched to the n_p, the m equals to 1 and the scattering turns out zero, thereby the OILC film is scattering-free. One more noticeable thing in general is that an extraordinary refractive index n_e of LC is much larger than n_p whereas an ordinary refractive index n_o of LC is very close to n_p. As we mentioned above, the existence of few droplets bigger than 350 nm with bipolar configuration causes to deviate the light propagation direction.

As mentioned already, the LC molecules inside droplets have a bipolar configuration in conventional-OILC. Therefore, an incident linearly polarized light at normal direction would experience different effective refractive indices n_{eff} depending on positions of LC director in droplets and its magnitude will vary from n_e to n_o of LCs. When the director is positioned parallel (perpendicular) to the substrate, the refractive index that the incident light experiences n_e (n_o), and when it is n_e, the m will be much larger than 1, giving rise to unwanted scattering. However, when it is n_o, the m will be close to 1, giving rise to minimal scattering. Even when the director is tilted to some angles to the substrate, n_{eff} of LC droplets will be still larger than n_p, i.e., m is still larger than 1, giving rise to some level of scattering. Finally, one can summarize two causes for unwanted scattering in OILC: large size of droplets over 200 nm and large ratio of m over 1.

By introducing a small amount of chiral dopant, the bipolar LC droplet would change to helical droplets. In this case, the twisted-OILC droplets possess a twist to the LC molecules. Here, the LC molecules possess the twist along the director, i.e., the nematic director curvature field generates twist with respect to the director. Therefore, the incident light experiences refractive index of LC droplets less than ne which is closer match to the n_p, which will reduce unwanted scattering. The schematic of twisted LC orientation inside the LC droplet has been shown in inset of Fig. 1(b).

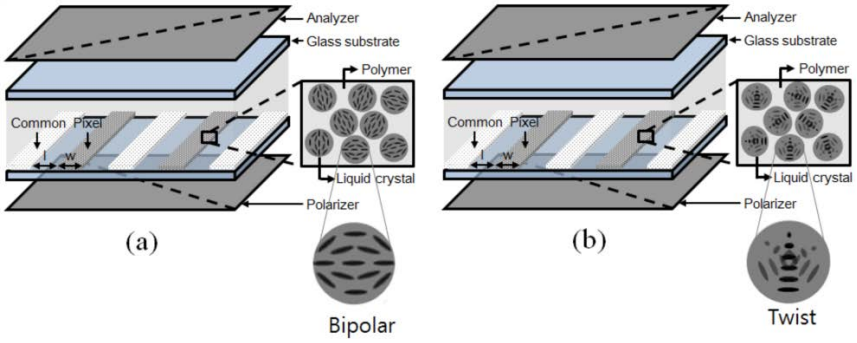

Fig. 1. Schematic diagram of the IPS cell with randomly oriented LC droplets in the (a) conventional-OILC phase, and (b) proposed twisted-OILC at field-OFF state. The bipolar LC and twisted LC orientation inside the droplets in conventional-OILC and twisted-OILC is shown in insert, respectively.

When the conventional-OILC is subjected to a strong electric field, the LC molecules inside the droplet tend to reorient along the field direction thus induced birefringence Δn_{ind} occurs [21]. This phenomenon can be explained by an adopted Kerr effect and can be expressed as [22], $\Delta n_{ind} = K\lambda E^2$. Here K is the Kerr constant and E is the applied electric field. Furthermore, at higher fields V = V_{op}, the LC molecules reorient along the field direction and saturates. This phenomenon can be precisely explained by the extended Kerr equation, expressed as [23],

Optics EXPRESS

$$\Delta n_{ind} = \Delta n_s \left\{ 1 - \exp\left[-\left(\frac{E}{E_s} \right)^2 \right] \right\}, \quad (2)$$

where Δn_s is the saturated birefringence and E_s is the saturated applied electric field. The Δn_{ind} equals to Δn_s as the E reaches E_s. It is worth to mention that the Kerr constant K is linearly proportional to the $\Delta\varepsilon$, Δn, and R [24].

In order to understand the electro-optical properties associated with helical pitch, we need to know the accurate pitch induced from the chiral dopants. The helical pitch length can be calculated from the equation,

$$P = \frac{1}{HTP \times c}, \quad (3)$$

where HTP is the helical twist power and c is the chiral dopant concentration [25].

3. Experiments

The prepared OILC film consists of a high dielectric anisotropy nematic LC mixture, a photo-curable monomer, and the chiral dopant. We utilized the MLC-2053 ($\Delta\varepsilon$ = 46.2 at 1 kHz, T_{NI} = 86°C, n_e = 1.7472, n_o = 1.5122, Δn = 0.235 at 589.3 nm, k_{11} = 13.2 pN, k_{22} = 6.5 pN, k_{33} = 18.3 pN, rotational viscosity (γ_1) = 123 mPa·s, from Merck Advanced Technology, Korea) as nematic LC, NOA 65 (Norland Optical Adhesive, n_p = 1.5275 at 20°C and 589 nm) as monomer, and SRM17 (helical twist power (HTP) = 166 μm^{-1}) as chiral dopant. We also added a small amount of photo-initiator, Irgacure-907, in order to initiate the polymerization.

We have prepared an OILC sample with 45 wt% of NLC and 55 wt% of NOA 65 and added various concentrations of the chiral dopant SRM17 to induce the twist to LC inside the droplets. The pitch length can be calculated by using a simple equation, Eq. (3). The detailed chiral dopant concentration and calculated pitch length have been shown in Table 1. The approximate material concentrations and curing conditions was chosen based on previous results, reported elsewhere [4,15,17–19]. Hereafter, the pitch length 0, 1.5, 1, 0.4, 0.3, and 0.2 μm samples are named as P1, P2, P3, P4, P5, and P6, respectively. Firstly, the electro-optical properties were studied as a function of UV curing intensity which is the most striking effect in the phase separation. Secondly, we studied the electro-optical properties as a function of pitch length. To check phase separation effect on electro-optics, we irradiated the sample P3 (1 μm) with various UV intensity. Later case, we fix the UV intensity for all the samples and characterized helical twist influence on OILC device. In order to avoiding intrinsic problems associated with phase separation, all the samples were irradiated without changing the duration of UV irradiation and sample's temperature which could play a crucial role on phase separation. After preparing the homogeneous mixture of NLC, monomer and chiral dopant, the mixture was filled into an IPS cell at slightly above the T_{NI} of NLC, 90°C, by capillary action. In the first case, the 1 μm pitch length sample, P3, was irradiated by 150, 140, 130 mW/cm^2 intensity UV light for 6 min. After careful evolution of the electro-optical properties, we fix the UV intensity 140 mW/cm^2 for 6 min curing time for all the samples and studied electro-optical properties as a function of pitch length.

The IPS cells employed in this report consist of indium tin oxide (ITO) coated comb like interdigitated electrodes on the bottom substrate while no electrodes on top substrate. Both the electrode width (w) and spacing (l) are fixed to 4 μm. The uniform gap (d) between two substrates is fixed to 10 μm by using a silicon ball spacer.

To investigate various properties of twisted-OILC, several characterization techniques have been performed namely the polarizing optical microscope (POM) (Nikon, ECLIPSE E600) with CCD camera (Nikon, DXM 1200) attached was used to identify and characterize the optically isotropic phase. The electro-optical properties were measured by using a lab-made experimental setup at which the IPS electrodes make 45° to the polarizer and the

Optics EXPRESS

analyzer fixed 90° to the polarizer. He-Ne laser (λ = 632.8 nm) light passing through the IPS cell and transmitted light detected by photo-diode which is connected to the digital oscilloscope (Tektronix, DPO 2024B). The electric field supplied to the IPS cell is generated by the function generator (Agilent, 33521A) and amplified by an amplifier (FLC Electronics, A400). The photographic images were taken by using a high resolution camera (Samsung, NX1000) under ambient light conditions. The wavelength-dependent transmittance was measured by using UV-Visible spectroscopy (SCINCO, S-3100) from ultraviolet to near infrared region. The POM images obtained at field-off state were utilized for measuring efficiency of black state by using *i*-solution software (*i*-Solution Inc., *i*M Technology). Finally, the LC was extracted from the cell and the polymer microstructure was characterized by using the field emission scanning electron microscope (FE-SEM).

Table 1. The OILC mixtures as a function of the various concentrations of chiral dopant

Sample Name	OILC[a], (wt%)	SRM17, (wt%)	Pitch Length (*P*), (μm)
P1	100	-	-
P2	99.6	0.4	1.5
P3	99.4	0.6	1
P4	98.5	1.5	0.4
P5	98	2	0.3
P6	97	3	0.2

[a]OILC is a mixer of MLC-2053:NOA 65 = 45:55 (wt%).

4. Results and discussion

We have chosen the 1 μm pitch length sample, P3, to study the phase separation influence on twisted-OILC as a function of UV curing intensity. We perform the phase separation with 130, 140, 150 mW/cm^2 intensity of UV light for 6 min. The POM images observed under different UV curing intensities were shown in Fig. 2(a), and corresponding dark state values were represented on each POM image. All exhibited an efficient black state, though the P3 with higher UV curing intensity, 150 mW/cm^2 showed the least light leakage. Voltage-dependent transmittance (V-T) were also measured as shown in Fig. 2(b) and the dark states were well kept even after voltage driving for all cases but V-T curves showed strong dependency on UV intensities. Even though, we achieved an efficient black state for 150 mW/cm^2 samples, the on-state transmittance was slightly reduced compared to that with 140 mW/cm^2. The data imply that UV curing intensity 130 mW/cm^2 is not enough for complete phase separation whereas 150 mW/cm^2 gives over exposure forming LC droplets too small. The formation of smaller nano-droplets which could not respond to the external field may be the reason for less on-state transmittance of 150 mW/cm^2 sample. By comparing all the samples, the 140 mW/cm^2 UV intensity is showing a maximum transmittance with an efficient black state. The threshold voltage (V_{th}) and operating voltage (V_{op}) are defined as the voltage corresponding to 10% and 90% transmittance, respectively. From the V-T curves, one can easily notice significant changes on both the V_{th} and V_{op} due to alteration in phase separation.

Hereafter, we fix the UV irradiation intensity 140 mW/cm^2 for 6 min for all the samples and characterized them as a function of pitch length. After phase separation, the wavelength dependent transmission was measured in the range from ultra-violet to visible region, as shown in Fig. 3(a). No polarizers are employed and measurements are performed at voltage-off state. From the UV-Visible transmission spectra, the transparency of the phase is gradually increasing from P1 to P6. It implies that matching degree of refractive index between the LC and polymer network is increasing as shortening the helical pitch. The increased in transmittance is measured as 10%, 16%, 24%, 29%, and 33% from P2 to P6, respectively, compared to conventional-OILC sample (P1). In addition, the transmission is also increasing with increasing in wavelength. According to RG scattering theory, Eq. (1), the

Optics EXPRESS

scattering intensity (σ) is inversely proportional to the wavelength of the incident light (λ^{-4}), which could be the reason for increasing transmission with wavelength [26].

We have taken high resolution photographic images for all the samples, obtained data illustrated in Fig. 3(b). The images were taken under ambient light condition without using polarizers. A noticeable light scattering was observed for conventional-OILC sample P1. However, the transparency of the phase seems to increase linearly for twisted-OILC samples from sample P1 to P6. The background characters are more clearly appearing for P6 that can be noticeable with necked eye.

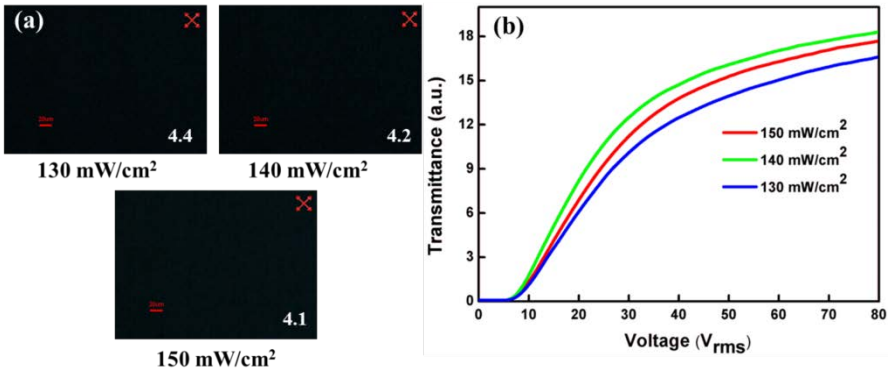

Fig. 2. (a) POM images and (b) voltage dependent transmittance, of 1 μm pitch length sample (P3) taken under crossed polarizers as a function of UV curing intensity. The scale bar in each POM images equals to 20 μm. The number on each POM image represents the black state.

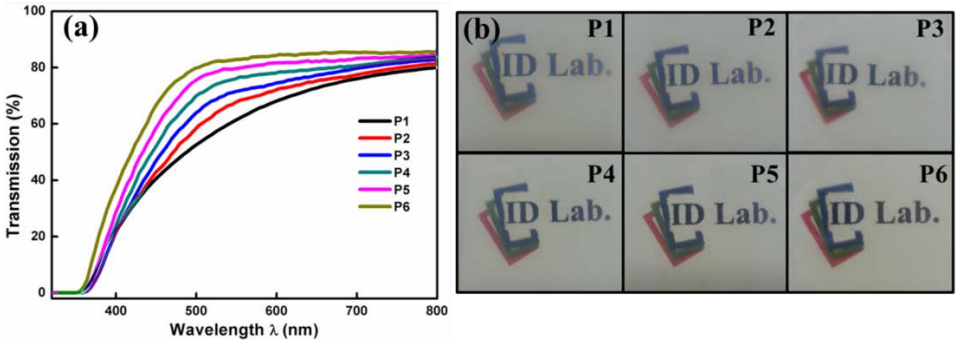

Fig. 3. (a) The wavelength dependent transmittance of prepares OILC samples measured by using UV-Visible spectroscopy, (b) The photographic images of cells.

In order to study the electro-optic properties associated with helical pitch, we have measured the V-T, as depicted in Fig. 4. Upon voltage application, the transmittance starts to increase after threshold voltage and get saturated at higher voltage. The pitch length dependent on-state transmittance of twisted-OILC is showing a mixed trend, compared to conventional-OILC, P1, as shown in Table 2. The saturated transmittance of longer pitch samples (P2 and P3) are increasing while the short pitch samples (P4, P5 and P6) are decreasing. A drastic improvement in on-state transmittance of P2 sample was noticed. When compared with conventional-OILC, P1, the saturation transmittance of P2 and P3 are increased by 49% and 39%, respectively. Overall, the pitch longer than the droplet size (R) are exhibiting higher transmittance and the pitch shorter than or equals to the droplet size (R) are showing less on-state transmittance. The small amount of chiral dopant concentration in P2 is creating a situation that all the LC molecules inside the droplet are responding to field, thereby achieved higher on-state transmittance. The LC molecules inside the droplets in a shorter pitch sample are not responding enough to applied electric field, which could be the

Optics EXPRESS

reason for less on-state transmittance. Therefore, the on-state transmittance is sequentially decreasing with decrease in pitch length.

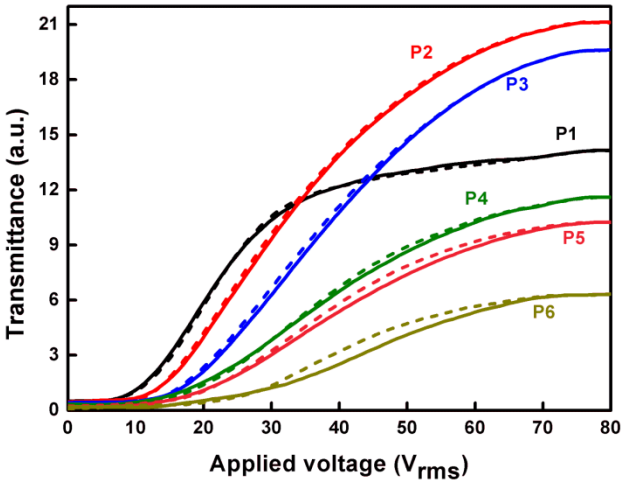

Fig. 4. The voltage-dependent transmittance curves of prepared samples. The solid lines indicate increasing of voltage and dotted lines indicates decreasing the voltage.

Table 2. The threshold voltage (V_{th}), hysteresis (H) and the change in transmittance as a function of pitch length.

Sample Name	V_{th} (V_{rms})	H (%)	Transmittance change[a] (%)
P1	12.9	0.22	-
P2	15.1	0.38	>49
P3	18.33	0.43	>39
P4	21.89	1.5	<18
P5	25.1	3.2	<27
P6	35.26	5.9	<55

[a]The > and < shows increased and decreased transmittance over the conventional-OILC, P1.

In general, the V_{th} and V_{op} for OILC are quite high as compared to other LC modes due to increased ratio of the effective surface area for LC anchoring to the effective volume within the droplet and field screening effect by the polymer. Consequently, one can expect that the twisted-OILC samples would also exhibit a higher V_{th} and V_{op}. As expected, the V_{th} and V_{op} are strongly influenced by the helical twist. In addition, the V_{th} is inversely proportional to the pitch length, i.e., shorter the pitch length then higher the V_{th}. In contrary, the V_{op} is not altered significantly with chiral dopant concentration.

Owing to twisted LC configuration, we adopted a threshold voltage relation from the conventional cholesteric liquid crystal. The V_{th} of twisted-OILC system must be varied with helical pitch length. The threshold voltage of the twisted LC with cell gap (d) can be expressed as [27,28],

$$V_{th} = \frac{d\pi^2}{P}\left(\frac{k_{22}}{\varepsilon_o \Delta\varepsilon}\right)^{1/2}, \quad (4)$$

where P is the helical pitch length of LC induced by chiral dopant, k_{22} is the twist elastic constant, ε_o is the free space dielectric permittivity and $\Delta\varepsilon$ is the dielectric anisotropy. From above equation, the V_{th} and the P are inversely proportional to each other. Consequently, the shorter pitch length causes to increase the V_{th} because the stronger helical twist demands the

Optics EXPRESS

higher voltage for unwinding the twist. Moreover, the surface anchoring energy induced by the polymer network also needed to overcome along with helical twist. Therefore, we conclude that the tendency of V_{th} could be due to stronger helical twisting power.

Furthermore, the hysteresis was also measured, from voltage dependent curves, which is one of the crucial parameter in OILCs. The hysteresis is defined as the voltage difference at 50% transmittance while increase and decreasing field swipes. The defined hysteresis can be mathematically expressed as,

$$H(\%) = \frac{\Delta V_{T50\%}}{V_{T100\%}} \times 100, \tag{5}$$

where $\Delta V_{T50\%}$ is the voltage difference between 50% transmittance while increasing and decreasing voltage, and $V_{T100\%}$ is the voltage corresponding to saturated transmittance. We have measured the hysteresis (%) from voltage-dependent voltage shown in Fig. 4, and the measured hysteresis values are shown in Table. 2. Interestingly, the hysteresis for the samples P2 (0.38%) and P3 (0.43%) is not much affected by the chiral dopant because the helical pitch is much longer than LC droplet. Due to insufficient helical twist, the LC molecules are more precisely followed to the applied electric field therefore achieved negligible hysteresis. In contrary, considerable hysteresis was noticed in shorter pitch length sample P4, P5, and P6. The measured hysteresis follows the order, P1<P2<P3<P4<P5<P6. It implies that the increase in helical twist causes to turn the nematic like phase to cholesteric like phase. The increase in chiral dopant concentration results in increase the tendency of cholesteric like phase formation, which could be the reason for hysteresis increase from P2 to P6.

The POM with crossed polarizers was used to characterize the voltage dependent switching properties of OILC. The back-light condition was kept constant all over the experiment to compare the samples one another. The isotropic nature was confirmed by rotating sample in sample's plane under crossed polarizers. When the sample was rotated on its plane at voltage-off state, no change in transmittance was noticed, which is the indication of optically isotropic phase. At off-state, all twisted-OILC samples exhibit an efficient isotropic phase unlike feeble scattering in the conventional-OILC (P1). In order to understand the efficiency of the dark state quantitatively, the voltage-off state optical images were analyzed by using an image analyzer software *i*-solution^{TM} where the perfect dark level is predefined as "0". The measured light leakages are 40.5, 4.2, 2.5, 1.5, 0.9 and 0.4 from P1 to P6, respectively. One can easily notice that the efficiency of the black state is drastically improved from P2 to P6, compared to conventional-OILC, P1. In addition, the tendency of black level is linearly increasing with decrease of pitch length. Since the UV curing condition and material concentration is unaltered, the variation in light leakage from sample to sample would be associated with LC molecular orientation inside the droplet. The chiral dopant which could modify the droplet structure bipolar to twisted configuration decreases the mismatching of refractive index between the LC/polymer networks. We also performed the optical switching measurements by supplying the voltage corresponding to peak voltage, as illustrated in Fig. 5. As expected, the on-state transmittance of twisted-OILC samples tends to decrease with pitch length. When compared with conventional-OILC sample P1, the transmittance of P2 and P3 are increased while P4, P5 and, P6 are decreased. The order of the on-state transmittance level follows, P2 (21.14) > P3 (19.62) > P1 (14.16) > P4 (11.59) > P5 (10.30) > P6 (6.28). The transmittance observed in the optical images is quite similar to the transmittance in V-T curves shown in Fig. 4. The small amount of chiral dopant resulted in drastic change in on-state transmittance in P2 and P3 because slightly induced twist reduces the scattering but still all the LC molecules inside the droplet respond to the field, thereby enhancing the induced birefringence. The shorter pitch length samples P4, P5, and P6 are unable to get maximum birefringence due to stronger helical twist which is having a less possibility to all the LC molecules responding to field. Therefore, one could easily anticipate

Optics EXPRESS

that the shorter helical pitch exhibits a less transmittance and, in addition, it requires higher V_{th}.

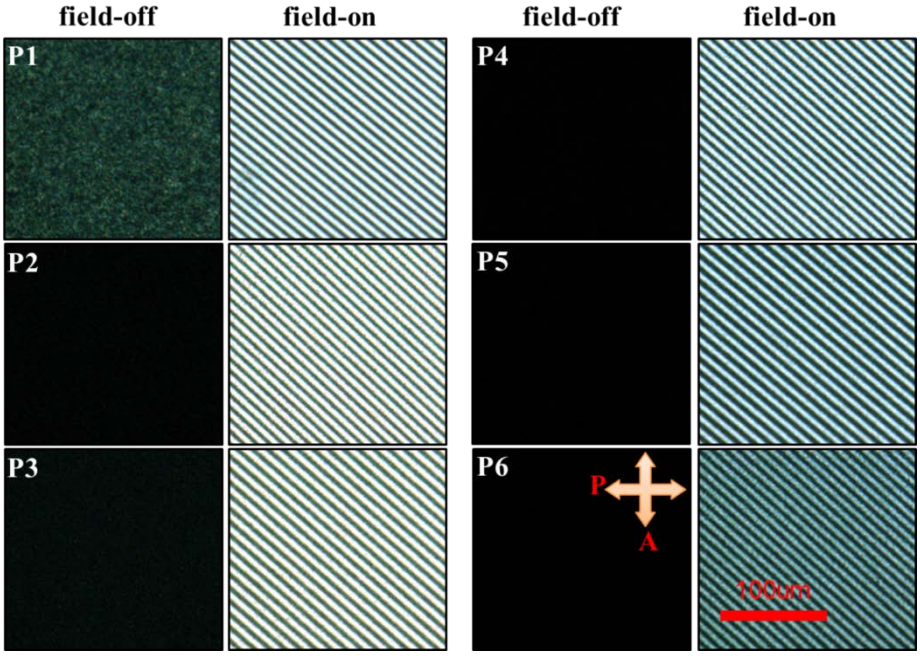

Fig. 5. The POM images of prepared sample at voltage-on and voltage-off states taken under crossed polarisers condition. The indicated scale bar equals to 100 μm. The crossed arrows represent orientation of polarizer and analyzer.

In order to quantitatively understand the helical pitch influence on performance on OILC phase, we have measured a light leakage and contrast ratio (CR). To measure light leakage and CR, we have used a visible (white) light and the cell was fixed between crossed polarizers. The long IPS electrodes are fixed to 45° with respect to the polarizer and the incident light propagates normal to the substrate. The CR is defined as the ratio between the intensity of light leakage at a zero voltage and transmitted light intensity at a saturated voltage. The light leakage is defined as the measured light leakage at voltage-off state under crossed polarizers. The light leakage and the CR are inversely proportional to each other. As shown in Fig. 6, the light leakage of twisted-OILC samples (P2 to P6) are drastically decreased, consequently, the CR enhanced. The light leakage in dark state was effectively reduced due to induced helical twist, because inducing a twist in the LC director inside the droplet gives rise to reduced effective LC refractive index so that the mismatch level in refractive index between LC droplet and polymer matrix is reduced. Even though the shorter pitch length samples (P4, P5, and P6) are exhibiting less on-state transmittance, the higher CR was achieved due to negligible (close to zero) light leakage. It suggests that the light leakage at off-state is a key parameter for improving the CR. The maximum CR, 1:1401, was achieved for 0.2 μm pitch length sample, P6, which is a competitive record among the similar literature [29,30].

Optics EXPRESS

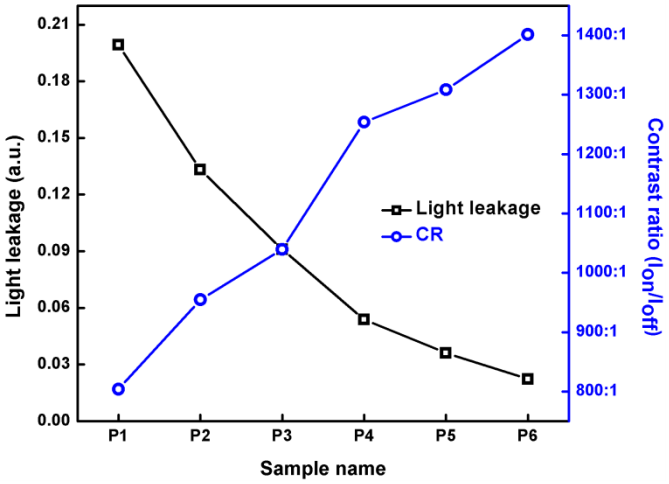

Fig. 6. The helical pitch length dependent light leakage and the contrast ratio measured under crossed polarizers.

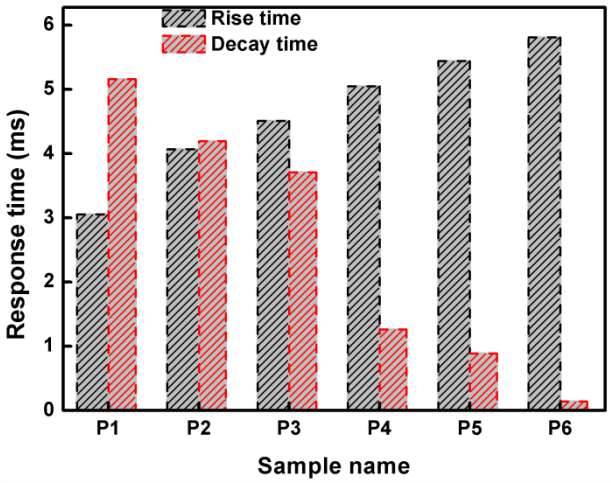

Fig. 7. The response times of the helical pitch length dependent samples measured with a maximum applied voltage of 80 V_{rms}.

Figure 7 shows the helical pitch influence on the response time. The response time was measured as the director response to saturated voltage, 80 V. The rise time is defined as the time for transmittance changes from 10% to 90% of maximum transmittance, and the decay time is the time that the transmittance changes from 90% to 10% of the maximum transmittance. The decay response time can be expressed as [28],

$$\tau_{off} \approx \frac{\gamma_1 R'^2}{k_{eff}\pi^2}, \tag{6}$$

where γ_1 is the rotational viscosity of the LC, k_{eff} is the effective elastic constant of LC, and R' is the resultant effect from both the droplet size and the pitch length. The Eq. (6) suggests that the decay response time is proportional to R'^2. Since the monomer to LC ratio is unaltered, the droplet size might not change. Therefore, the response time variation is purely from pitch length change. From Fig. 7, both the τ_{on} and τ_{off} are strongly affected by the pitch length. The τ_{on} is increased with decrease of pitch length while the τ_{off} is decreased. We infer that the stronger electric torque associated to the chiral dopant would require unwinding the helical

Optics EXPRESS

twist, thus τ_{on} is increased form P2 to P6. The measured decay response times were 4.2, 3.7, 1.3, 0.9, and 0.1 ms for P2, P3, P4, P5, and P6, respectively, all faster than that of the conventional-OILC sample (P1). Even though the decay response time can be improved further with shorter pitch, the other electro-optic properties such as operating voltage and transmittance require to be sacrificed.

In conventional-OILC, the LC droplets typically exhibit a bipolar configuration in which the nematic director field possesses a curvature at droplet boundary, and the curvature linearly decreases to zero towards bulk. The bipolar configuration shows a splay elastic distortion (k_{11}) in the vicinity of each defect and a bend elastic distortion (k_{33}) throughout the rest of the droplet. When a strong electric field is applied, at first all the directors pull towards the electric field and then the LC molecules inside the droplet reorient along the field direction. This two-step phenomenon in nano-sized droplets was explained by Chang et al. [18]. After field removal, the director relaxes to the previous position at which the visco-elastic coefficient (γ_1/k_{eff}) would be a driving factor. Here, the bend (k_{33}) and splay (k_{11}) elastic constants would contribute simultaneously to k_{eff} in Eq. (6).

In the second case, the twisted-OILC droplets possess a twist, associated with chiral dopant, while sustaining the bipolar structure. The nematic director field generates twist to the LC molecules inside the droplet. The effective elastic constant k_{eff} is approximately equal to average of $k_{11} + k_{22} + k_{33}$ for twisted-OILC whereas only $k_{11} + k_{33}$ contribute in conventional-OILC. The high chiral dopant concentration can induce the strong helical twist k_{22}, and consequently increases the k_{eff} for short pitch length samples (P4, P5, and P6). Therefore, the stronger electric torque is required to unwinding the twist when field is applied. On field withdrawn, the director relaxation, i.e., decay response time, depends on the k_{eff} and as well as pitch length. Therefore, we strongly emphasize that the resultant effect of large k_{eff} and shorter pitch length could be the reason behind the fast decay response of short pitch sample (P4, P5, and P6).

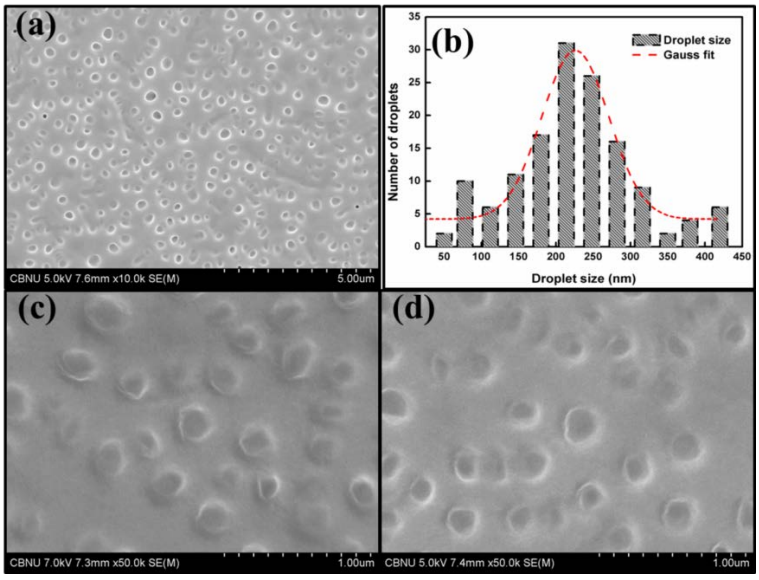

Fig. 8. (a) FE-SEM micro-images of the conventional-OILC, and (b) its size distribution with Gaussian fit. (c) and (d) are polymer micro-structure of twisted-OILCs with the helical pitch of 1.5 µm and 0.3 µm, respectively.

Finally, the polymer microstructure was characterized by using the FE-SEM after extracting the LC from the OILC film. The examined cells were soaked in n-hexane for 48 hrs to extract the LC from polymer network. After confirming the complete LC is extracted,

Optics EXPRESS

the two substrates were separated with sharp-edged blade. A thin conductive platinum film was coated over the polymer surface by RF sputtering to avoid the charge accumulation on polymer network. No tilt was made to the cell and the micro-images were taken normal to the substrate. The obtained image of sample P1 has been shown in Fig. 8(a). The average droplet size and the size distribution were estimated by using an image analyzer software, Image-J (a Java-based Image processing developed at the National Institute of Health), and obtained data was illustrated in Fig. 8(b). Majority of the droplets were found to be isolated and spherical shaped. The size distribution was analyzed by fitting to Gaussian function and the average droplet size was found to be 225 nm. The optically isotropic nature was attained from smaller droplets below the visible wavelength regime. A feeble light scattering is resulted from a few droplets bigger than 350 nm, which causes to the refractive index mismatch with polymer network. This could be one of the prime evidence for slight light scattering in conventional-OILC sample. Besides, a few LC droplets, those are smaller than 100 nm, demands a higher V_{th}. Figures 8(c) and 8(d) reveals that the chiral dopant does not show much effect on either the droplet size or the polymer network architecture. Since the monomer to LC ratio was unchanged, the droplet size might not change for twisted-OILC sample. By adding small amount of the chiral dopant to the conventional-OILC, the light leakage was effectively suppressed. Therefore, we confirm that the helical twist associated to chiral dopant is the reason for improved electro-optical properties of OILC device.

5. Conclusion

In summary, we have demonstrated an efficient OILC phase in which LC directors inside droplets are twisted, which is capable of reducing the light scattering. The electro-optic properties of the OILCs associated with helical pitch were studied in detail. The proposed device is exhibiting an outstanding dark state, and thus the CR was greatly improved. As the pitch decreases CR was increased, achieving high value 1401:1 for the helical pitch of 0.2 µm. In addition, the decay response time of the device is also greatly improved by introducing chiral dopant. Interestingly, tremendous improvement in on-state transmittance (49%) was achieved for 1.5 µm pitch length sample compared to conventional OILC. The reported high CR and high transmittance would be applicable to develop in the upcoming future flexible display and various photonic applications.

Funding

Basic Science Research Program through National Research Foundation of Korea (NRF) Ministry of Education (2016R1A6A3A11930056, 2016R1D1A1B01007189).

References

1. M. S. Kim, Y. J. Lim, S. Yoon, S. W. Kang, S. H. Lee, M. Kim, and S. T. Wu, “A controllable viewing angle LCD with an optically isotropic liquid crystal,” J. Phys. D Appl. Phys. **43**(14), 145502 (2010).
2. S. W. Choi, S. I. Yamamoto, T. Iwata, and H. Kikuchi, “Optically isotropic liquid crystal composite incorporating in-plane electric field geometry,” J. Phys. D Appl. Phys. **42**(11), 112002 (2009).
3. B. Bahadur, Liquid crystals: applications and uses. (World Scientific, 1990), Vol. **1**.
4. N. H. Park, S. C. Noh, P. Nayek, M. H. Lee, M. S. Kim, L. C. Chien, J. H. Lee, B. K. Kim, and S. H. Lee, “Optically isotropic liquid crystal mixtures and their application to high performance liquid crystal devices,” Liq. Cryst. **42**(4), 530–536 (2015).
5. L. Rao, Z. Ge, S. T. Wu, and S. H. Lee, “Low voltage blue-phase liquid crystal displays,” Appl. Phys. Lett. **95**(23), 231101 (2009).
6. Y. C. Yang and D. K. Yan, “Electro-optic Kerr effect in polymer-stabilized isotropic liquid crystals,” Appl. Phys. Lett. **98**(2), 023502 (2011).
7. H. Kikuchi, M. Yokota, Y. Hisakado, H. Yang, and T. Kajiyama, “Polymer-stabilized liquid crystal blue phases,” Nat. Mater. **1**(1), 64–68 (2002).
8. F. Castles, F. V. Day, S. M. Morris, D. H. Ko, D. J. Gardiner, M. M. Qasim, S. Nosheen, P. J. Hands, S. S. Choi, R. H. Friend, and H. J. Coles, “Blue-phase templated fabrication of three-dimensional nanostructures for photonic applications,” Nat. Mater. **11**(7), 599–603 (2012).
9. H. Choi, H. Higuchi, and H. Kikuch, “Fast electro-optic switching in liquid crystal blue phase II,” Appl. Phys. Lett. **98**(13), 131905 (2011).

Optics EXPRESS

10. Y. Haseba, H. Kikuchi, T. Nagamura, and T. Kajiyama, "Large electro-optic Kerr effect in nanostructured chiral liquid-crystal composites over a wide temperature range," Adv. Mater. **17**(19), 2311–2315 (2005).
11. S. Aya, K. V. Le, F. Araoka, K. Ishikawa, and H. Takezoe, "Nanosize-induced optically isotropic nematic phase," Jpn. J. Appl. Phys. **50**(5R), 051703 (2011).
12. J. L. West, "Phase separation of liquid crystals in polymers," Mol. Cryst. Liq. Cryst. Inc. Nonlinear Opt. **157**(1), 427–441 (1988).
13. R. S. Justice, D. W. Schaefer, R. A. Vaia, D. W. Tomlin, and T. J. Bunning, "Interface morphology and phase separation in polymer-dispersed liquid crystal composites," Poly. **46**(12), 4465–4473 (2005).
14. S. Matsumoto, M. Houlbert, T. Hayashi, and K. I. Kubodera, "Fine droplets of liquid crystals in a transparent polymer and their response to an electric field," Appl. Phys. Lett. **69**(8), 1044–1046 (1996).
15. S. J. Shin, N. H. Cho, Y. J. Lim, P. Nayek, S. H. Lee, S. H. Hong, H. J. Lee, and S. T. Shin, "Optically isotropic liquid crystal mixture showing high contrast ratio and fast response time," IMID Digest. 139–140 (2011).
16. Z. J. Lu and D. K. Yang, "Effect of chiral dopant on the performance of polymer dispersed liquid crystal light valve," Appl. Phys. Lett. **65**(4), 505–507 (1994).
17. J. H. Yu, H. S. Chen, P. J. Chen, K. H. Song, S. C. Noh, J. M. Lee, H. Ren, Y. H. Lin, and S. H. Lee, "Electrically tunable microlens arrays based on polarization-independent optical phase of nano liquid crystal droplets dispersed in polymer matrix," Opt. Express **23**(13), 17337–17344 (2015).
18. C. M. Chang, Y. H. Lin, V. Reshetnyak, C. H. Park, R. Manda, and S. H. Lee, "Origins of Kerr phase and orientational phase in polymer-dispersed liquid crystals," Opt. Express **25**(17), 19807–19821 (2017).
19. R. Manda, S. Pagidi, S. S. Bhattacharyya, C. H. Park, Y. J. Lim, J. S. Gwag, and S. H. Lee, "Fast response and transparent optically isotropic liquid crystal diffraction grating," Opt. Express **25**(20), 24033–24043 (2017).
20. G. P. Montgomery, Jr., J. L. West, and W. Tamura-Lis, "Light scattering from polymer-dispersed liquid crystal film: droplet size effects," J. Appl. Phys. **69**(3), 1605–16012 (1991).
21. J. Niziol, R. Weglowski, S. J. Klosowicz, A. Majchrowski, P. Rakus, A. Wojciechowski, I. V. Kityk, S. Tkaczyk, and E. Gondek, "Kerr modulators based on polymer-dispersed liquid crystal complexes," J. Mater. Sci. Mater. Electron. **21**(10), 1020–1023 (2010).
22. J. Kerr, "A new relation between electricity and light: Dielectrified media birefringent," J. Sci. **50**(332), 337–348 (1875).
23. J. Yan, L. Rao, M. Jiao, Y. Li, H. C. Cheng, and S. T. Wu, "Polymer-stabilized optically isotropic liquid crystals for next-generation display and photonics applications," J. Mater. Chem. **21**(22), 7870–7877 (2011).
24. P. R. Gerber, "Electro-optical effects of a small-pitch blue-phase system," Mol. Cryst. Liq. Cryst. (Phila. Pa.) **116**(3–4), 197–206 (1985).
25. M. R. Wilson and D. J. Earl, "Calculating the helical twisting power of chiral dopants," J. Mater. Chem. **11**(11), 2672–2677 (2001).
26. S. Zumer and J. W. Doane, "Light scattering from a small nematic droplet," Phys. Rev. A Gen. Phys. **34**(4), 3373–3386 (1986).
27. R. B. Meyer, "Effects of electric and magnetic fields on the structure of cholesteric liquid crystals," Appl. Phys. Lett. **12**(9), 281–282 (1968).
28. M. Oh-e and K. Kondo, "Response mechanism of nematic liquid crystals using the in-plane switching mode," Appl. Phys. Lett. **69**(5), 623–625 (1996).
29. R. Manda, S. Pagidi, M. S. Kim, C. H. Park, H. S. Yoo, K. Sandeep, Y. J. Lim, and S. H. Lee, "Effect of monomer concentration and functionality on electro-optical properties of polymer-stabilised optically isotropic liquid crystals," Liq. Cryst. **45**(5), 736–745 (2018).
30. N. H. Cho, P. Nayek, J. J. Lee, Y. J. Lim, J. H. Lee, S. H. Lee, H. S. Park, J. H. Lee, and H. S. Kim, "High-performance, in-plane switching liquid crystal device utilizing an optically isotropic liquid crystal blend of nanostructured liquid crystal droplets in a polymer matrix," Mater. Lett. **153**, 136–139 (2015).